Int. J. Multiphase Flow Vol. 12, No. 6, pp. 891–912, 1986
Printed in Great Britain

0301-9322/86 $3.00 + 0.00
Pergamon Journals/Elsevier

NONSPHERICAL PARTICLES IN TWO-PHASE FLOW

D. BESNARD†
Centre d' Etudes de Limeil, B.P. 27, 94190 Villeneuve-St-Georges, France

F. H. HARLOW
Los Alamos National Laboratory, Los Alamos, NM 87545, U.S.A.

(*Received* 2 *August* 1985; *in revised form* 5 *February* 1986)

Abstract—We have examined the two-phase flow of a gas with dispersed, nonspherical, rigid particles. We describe a model for the motion of a single ellipsoid in the fluid, including the degrees of freedom associated with translation, lift, orientation and angular velocity. We assume there is no interaction between the particles, and give the Liouville equation for the distribution function of the particles. A computer code has been developed to simulate the two-dimensional behavior of such a flow. We demonstrate, in the case of a high-speed jet impinging on an obstacle, that the force exerted on the obstacle by the particles depends strongly on the eccentricity.

1. INTRODUCTION

The presence of particles in a flow can alter both its dynamics and thermodynamics, depending on the volume fraction α_1 of the particles, their size and their density. For $\alpha_1 > 0.2$, particle collisions become an important phenomenon. At the close packing limit ($\alpha_1 = 0.45$ for spheres), the two-field flow behavior is characterized by the effect of the collisions between the particles rather than by any other interaction between the surrounding fluid and the particles. For small values of α_1, collision effects can be neglected, and the flow regime is characterized by interactions between the fluid and each of the particles.

Consider a single particle. The forces acting on this particle can be isolated (see Jeffery 1922; Lamb 1966). If the Reynolds number $\mathrm{Re} \ll 1$, the particle is mainly subject to Stokes drag in steady state. A nonspherical particle is also subject to a lift and a torque created by the difference of fluid microscopic velocity on its surface. If $\mathrm{Re} > 5$, we have to consider a form of drag as well as a flow separation lift. If $\mathrm{Re} > 40$, turbulent eddies are produced in the shedding vortex sheet downstream of the particle. For nonsteady flows, a representation of the force acting on a spherical particle can be expressed as the sum of the Stokes drag and the history-dependent Basset term. A considerable amount of work has already been done in the case of spherical particles in a fluid by Margolin (1977). However, the assumption of sphericity is often far from reality. A theoretical investigation has been performed by Jeffery (1922) in the case of ellipsoids. Also, experiments have been performed by Goldsmith & Mason (1962) on suspensions of ellipsoids in tubes. Both are low-speed studies; our goal is to derive a more general model, which holds for both high- and low-speed flows. One of our motivations is to be able to describe the flow of high-speed jets with entrained nonspherical particles, for application to some nuclear reactor safety problems. An example is the jet produced by the rupture of a tube in which pressurized water circulates. Another motivation is to describe the two-field flow of solid particles (e.g. sand grains) blown away by a shock. For simplicity, we assume that the particle shapes are ellipsoids.

In section 2 we propose a heuristic model describing the different forces acting on a single particle due to the action of the surrounding fluid. Because we are mostly interested in the collective behavior of the particles in the fluid, this model is not a detailed description of the interaction between a single particle and the surrounding fluid. However, it gives

†Visiting Staff Member, Los Alamos National Laboratory.

expressions for drag, lift and torque at any flow speed. The model also allows us to calculate characteristic times (e.g. rotation time). Although we only consider rigid particles at the present stage of our study, we determine in section 2 in which regime the deformation of the particle is important, compared to their rotation. Besides mechanical actions, we also have thermodynamic processes, such as the heat transfer between the particle and the surrounding fluid, and the compression of both the particle and the fluid. Due to the relative incompressibility of the particle, heat transfer can be much faster within the particles than in the fluid and the energy released to the fluid may be very important for a given volume of fluid, if the density of the particles is much larger than the density of the fluid. To take these actions into account, it is necessary to know certain coefficients such as the rate of thermal change between the fluid and the particles, and the characteristics of the material constituting the particles. For simplicity, we neglect such processes in this paper; their effect will be considered in a subsequent paper.

We use the results of section 2 to derive a model for a two-field flow composed of ellipsoidal particles entrained in a fluid. The fluid equations for a two-field flow have been derived by many investigators, usually by considering microscopic conservation equations for mass, momentum and energy, and integrating these equations over some control volume (see Nigmatulin 1979). There are some conceptual difficulties in the manner in which cuts are made through the material of one field in order to integrate over the other, and in the way area and volume integrals over a single phase are transformed to integrals over the entire control volume. Also, there are some difficulties due to the fact that using fluid equations for a dispersed phase means that one assumes the distribution function of the particles to be Maxwellian in velocity. Thus, the detailed description of the distribution function is lost. In order to preserve the local spectra of velocity, angular velocity and orientation of the particles, we employ in section 3 a Liouville equation to describe the distribution of the dispersed phase in physical, velocity and orientation space. This approach forms a consistent basis for complicated extensions to the field equations, such as the effect of a non-Maxwellian velocity distribution for the particles, and the introduction of turbulence.

We describe in section 3 a hybrid model, consisting of this Liouville equation for the particles, which uses the results of section 2 coupled with field equations for the surrounding fluid. We briefly consider the introduction of turbulence into our model, and its effect on the Liouville equation.

To illustrate the possibilities of this model, a code has been developed to obtain solutions for the model in a 2-D plane geometry. In section 4, we present numerical results for the special case of high-speed jets. We study the behavior of a jet impinging on a rectangular obstacle, and the influence of particle eccentricity on the pressure exerted on the obstacle.

2. BEHAVIOR OF AN ELLIPSOIDAL PARTICLE IN A FLUID

2.1. Modeling requirements

We consider here an ellipsoid, of principal radii a and b, with $b < a$ (see figure 1). We also define the normal $\mathbf{n}$ to the surface of largest cross section at its center of mass, and the two angles ξ and β, such that

$$\xi = (\mathbf{n}, \mathbf{x}), \tag{1}$$

where $(\mathbf{x})$ is in the laboratory frame, and

$$\beta = (\mathbf{n}, \mathbf{u}_2 - \mathbf{u}_1), \tag{2}$$

where $\mathbf{u}_1$ is the particle velocity, and $\mathbf{u}_2$ is a mean fluid velocity at the same location as the particle. If the particles are much smaller than our length scale of interest, we also might define the velocity $\mathbf{u}_2$ as an ensemble average of the microscopic velocities of the fluid over a control volume in phase space (see Nigmatulin 1979). Starting from the work of other investigators (e.g. for spherical particles), we seek a simple extension to ellipsoids.

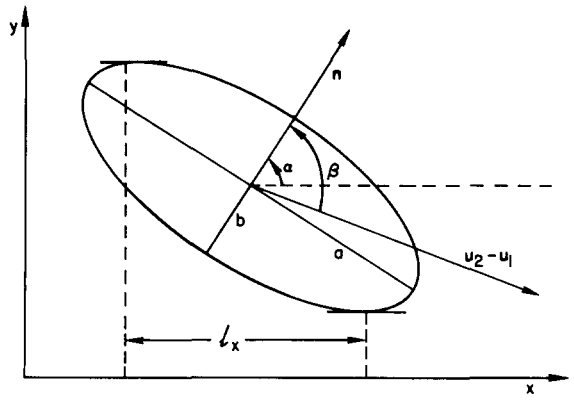

Figure 1. Ellipsoid in a fluid.

The heuristic requirements for obtaining our expressions are that:

(1) The different symmetries in the problem are respected.
(2) The expressions are tensor invariant.
(3) The limiting cases are recovered. If $a = b$, i.e. if the particle is spherical, we do not have rotation nor lift of the particle. Likewise, for an infinitely massive particle, there is no motion; if $\beta = \pi/2$, there is no torque; and if β vanishes, there is no lift.
(4) Dimensionality properties are respected.
(5) The different coefficients are deduced, if possible, from known coefficients for spherical particles.
(6) We choose the simplest linear or quadratic expressions satisfying the above requirements.

2.2. Drag force

At steady state, when $\mathrm{Re} \ll 1$, we have (see Chandrasekhar 1943)

$$\mathbf{F}_D = 6\pi\eta R(\mathbf{u}_2 - \mathbf{u}_1), \qquad [3]$$

where R is the radius of a spherical particle and η is the viscosity of the surrounding fluid. According to our requirements, we propose

$$\mathbf{F}_{D1} = K_{D1}\eta V_p^{1/3}(\mathbf{u}_2 - \mathbf{u}_1), \qquad [4]$$

where V_p is the volume of the particle. For high-speed flows, the usual expression (see Daly & Harlow 1978) is

$$\mathbf{F}_D = K\rho_2\pi R^2|\mathbf{u}_2 - \mathbf{u}_1|^2. \qquad [5]$$

We propose here,

$$\mathbf{F}_{D2} = K_{D2}\rho_2 S_{\mathrm{eff}}|\mathbf{u}_2 - \mathbf{u}_1|(\mathbf{u}_2 - \mathbf{u}_1), \qquad [6]$$

where $S_{\mathrm{eff}} = \pi a^2(\cos^2\beta + e^2\sin^2\beta)^{1/2}$ is the cross section of the particle with respect to $\mathbf{n}$, and $e = b/a$ is the particle eccentricity.

2.3. Lift force

The lift force is orthogonal to the vector $\mathbf{U} = \mathbf{u}_2 - \mathbf{u}_1$ and in our case lies in the plane defined by the vectors $\mathbf{n}$ and $\mathbf{U}$. The expression for the lift must be invariant under a 180° rotation of the particle, and vanishes if $\beta = \pi/2$. We thus propose

$$\mathbf{F}_{L1} = C_{L1}[-\mathrm{sign}(\mathbf{n}\cdot\mathbf{U})]\left(\mathbf{n} \times \frac{\mathbf{U}}{|\mathbf{U}|}\right) \times \mathbf{U} \qquad [7]$$

for Stokes lift and

$$\mathbf{F}_{L2} = C_{L2}[-\text{sign}(\mathbf{n}\cdot\mathbf{U})](\mathbf{n}\times\mathbf{U})\times\mathbf{U}, \tag{8}$$

for flow-separation lift.

Define

$$A(\beta) \equiv (\cos^2\beta + e^2\sin^2\beta)^{1/2} \quad \text{and} \quad B(\beta) \equiv (e^2\cos^2\beta + \sin^2\beta)^{1/2}.$$

We propose the following expressions for the coefficients C_{L1} and C_{L2}:

$$C_{L1} = K_{L1}\eta(a-b) \tag{9}$$

and

$$C_{L2} = \tfrac{1}{2}K_{L2}\rho_1 l_x a, \tag{10}$$

where l_x is defined in figure 1. We have

$$l_x = \frac{a(1-e^2)|\sin^2\beta|}{B(\beta)}.$$

Thus

$$C_{L2} = \frac{\tfrac{1}{2}K_{L2}\rho_2(a^2-b^2)|\sin^2\beta|}{B(\beta)}. \tag{11}$$

In summary, the equation of motion for the particle is

$$\begin{aligned} m\frac{d\mathbf{u}_1}{dt} = &-V_p\nabla P_2 + K_{D1}\eta V_p^{1/3}(\mathbf{u}_2-\mathbf{u}_1) + K_{D2}\rho_2 S_{\text{eff}}|\mathbf{u}_2-\mathbf{u}_1|(\mathbf{u}_2-\mathbf{u}_1) \\ &+ C_{L1}\left[\mathbf{n}\times\frac{(\mathbf{u}_2-\mathbf{u}_1)}{|\mathbf{u}_2-\mathbf{u}_1|}\right]\times(\mathbf{u}_2-\mathbf{u}_1)\{-\text{sign}[\mathbf{n}\cdot(\mathbf{u}_2-\mathbf{u}_1)]\} \\ &+ C_{L2}[\mathbf{n}\times(\mathbf{u}_2-\mathbf{u}_1)]\times(\mathbf{u}_2-\mathbf{u}_1)\{-\text{sign}[\mathbf{n}\cdot(\mathbf{u}_2-\mathbf{u}_1)]\}, \end{aligned} \tag{12}$$

where P_2 is the fluid pressure. The coefficients K_{D1}, K_{D2}, K_{L1} and K_{L2} are constants of the order of unity.

2.4. Torque

We consider four different contributions to the torque acting on one particle. The first is the viscous damping of the vorticity of the surrounding fluid, and the second is the flow-separation damping. The source of vorticity is $\frac{1}{2}\nabla\times\mathbf{u}_2$, and we thus propose

$$\mathbf{T}_1 = K_{\omega 1}\eta V_p(\tfrac{1}{2}\nabla\times\mathbf{u}_2 - \boldsymbol{\omega}) \tag{13}$$

and

$$\mathbf{T}_2 = \tfrac{1}{2}K_{\omega 2}\rho_2 a(a-b)S_p A(\beta)|\mathbf{u}_2-\mathbf{u}_1|(\tfrac{1}{2}\nabla\times\mathbf{u}_2-\boldsymbol{\omega}), \tag{14}$$

where $\boldsymbol{\omega}$ is the angular velocity of the particle, and

$$S_p = \pi a^2.$$

The two other contributions to the torque acting on the particle result from the nonsymmetric repartition of the microscopic fluid velocities on the surface of the particle. Such terms must vanish if $\mathbf{u}_2-\mathbf{u}_1$ is orthogonal or parallel to $\mathbf{n}$. Thus, we propose

$$\mathbf{T}_3 = -K_{\omega 3}\eta b(a-b)\left(\mathbf{n}\cdot\frac{\mathbf{u}_2-\mathbf{u}_1}{|\mathbf{u}_2-\mathbf{u}_1|}\right)[\mathbf{n}\times(\mathbf{u}_2-\mathbf{u}_1)] \tag{15}$$

for the viscous torque and

$$\mathbf{T}_4 = \tfrac{1}{2}K_{\omega 4}\rho_2(a-b)S_p[\mathbf{n}\cdot(\mathbf{u}_2-\mathbf{u}_1)][\mathbf{n}\times(\mathbf{u}_2-\mathbf{u}_1)] \tag{16}$$

for the flow-separation torque. The resulting equation for the variation of angular velocity

of the particle is

$$\mathbb{J}:\frac{d\boldsymbol{\omega}}{dt} = K_{\omega 1}\eta V_p(\tfrac{1}{2}\nabla \times \mathbf{u}_2 - \boldsymbol{\omega}) + \tfrac{1}{2}K_{\omega 2}\rho_2 a(a-b)S_p A(\beta)|\mathbf{u}_2 - \mathbf{u}_1|(\tfrac{1}{2}\nabla \times \mathbf{u}_2 - \boldsymbol{\omega})$$
$$-\mathbf{K}_{\omega 3}\eta b(a-b)\left(\mathbf{n}\cdot\frac{\mathbf{u}_2-\mathbf{u}_1}{|\mathbf{u}_2-\mathbf{u}_1|}\right)[\mathbf{n}\times(\mathbf{u}_2-\mathbf{u}_1)]$$
$$+\tfrac{1}{2}K_{\omega 4}\rho_2(a-b)S_p[\mathbf{n}\cdot(\mathbf{u}_2-\mathbf{u}_1)][\mathbf{n}\times(\mathbf{u}_2-\mathbf{u}_1)], \qquad [17]$$

where $\mathbb{J}$ is the moment of inertia of the particle. The coefficients $K_{\omega 1}$, $K_{\omega 2}$, $K_{\omega 3}$ and $K_{\omega 4}$ are constants of the order of unity.

2.5. Relaxation times

Equations [12] and [17] exhibit characteristic times of interest, such as a rotation time, and a relaxation time for the equilibrium orientation of the particle with respect to the fluid velocity $\mathbf{u}_2$, and consequently a vanishing time for the lift velocity. Also of interest is the relaxation time of $\mathbf{u}_1$ towards $\mathbf{u}_2$. We compare here rotation time with deformation time, to determine in which range of parameters this modeling is valid.

First, assuming that $\mathbf{u}_1$ and $\mathbf{u}_2$ are constant velocities, we choose the first axis of the inertial frame to coincide with $\mathbf{u}_2 - \mathbf{u}_1$. Restricting ourselves to low-speed flows, [17] becomes, with $\dot{\xi} = \omega$,

$$\mathbb{J}\ddot{\xi} = -C_{\omega 1}\dot{\xi} - C_{\omega 3}\sin\xi\cos\xi$$

or, for small oscillations around $\xi = 0$,

$$\mathbb{J}\ddot{\xi} = -C_{\omega 1}\dot{\xi} - C_{\omega 3}\xi, \qquad [18]$$

where $C_{\omega 1}$ and $C_{\omega 3}$ are independent of ξ. This equation admits exponentially decreasing solutions, which shows that $\xi = 0$, $\omega = 0$ is a stable equilibrium position. Conversely, around $\xi = \pi/2$, $\omega = 0$, [17] can be written as

$$\mathbb{J}\ddot{\xi} = -C_{\omega 1}\dot{\xi} + C_{\omega 3}\xi, \qquad [19]$$

which leads to solutions whose stability depends on the balance between the speed of the surrounding flow and the strength of the damping rate.

If the particles are not solid, rotation competes with deformation. From [18] or [19], an estimation of the time for which a significant rotation of the particle takes place is $\delta t_r = (\mathbb{J}C_{\omega 3}^{-1})^{1/2}$. It is proportional to $|\mathbf{u}_2 - \mathbf{u}_1|^{1/2}$ for Stokes flow, and to $|\mathbf{u}_2 - \mathbf{u}_1|$ for inertia-dominated flow. The deformation time can be estimated by balancing internal and external stresses acting on the particle. For inertia-dominated deformation, we can estimate the internal stress to be $2\eta_1\mathbf{u}_d/r$ ($\mathbf{u}_d$ is the distortion velocity and η_1 is the viscosity of the material of which the particle is constituted), and the external stress to be $\frac{1}{2}\rho_2|\mathbf{u}_2 - \mathbf{u}_1|^2$. Thus $\mathbf{u}_d \simeq r\rho_2|\mathbf{u}_2 - \mathbf{u}_1|^2/4\eta_1$, and the distortion time $\delta t_d \simeq r/\mathbf{u}_d$ is $\delta t_d \simeq 4\eta_1/\rho_2|\mathbf{u}_2 - \mathbf{u}_1|^2$. For viscous-dominated deformation, the same balance leads to the equation

$$\frac{d}{dt}\left(\frac{4\pi}{3}r^3\rho_1\mathbf{u}_d\right) = \tfrac{1}{2}\rho_2|\mathbf{u}_2 - \mathbf{u}_1|^2\pi r^2.$$

In terms of the distortion amplitude a_d, where $da_d/dr = \mathbf{u}_d$, we obtain $d^2a_d/dt^2 = 3\rho_2(\mathbf{u}_2 - \mathbf{u}_1)^2/8\rho_1 r$, and thus, taking $a_d = r$, $\delta t_d \approx [3\rho_2(\mathbf{u}_2 - \mathbf{u}_1)^2/8\rho_1 r^2]^{-1/2}$. Hence, for low-speed flows,

$$\delta t_r \propto (\mathbf{u}_2 - \mathbf{u}_1)^{-1/2}$$

and

$$\delta t_d \propto (\mathbf{u}_2 - \mathbf{u}_1)^{-1}. \qquad [20]$$

For high-speed flows,

$$\delta t_r \propto (\mathbf{u}_2 - \mathbf{u}_1)^{-1}$$

and

$$\delta t_d \propto (\mathbf{u}_2 - \mathbf{u}_1)^{-2}. \quad [21]$$

Equations [20] and [21] indicate that, for fluid particles, the rotation time is smaller for large velocities, and larger for small velocities than the distortion time. This indicates the necessity of including deformation in any model dealing with fluid particles.

We now analyze the relaxation of $\mathbf{u}_1$ towards $\mathbf{u}_2$. Equation [12], in 1-D plane geometry, and without lift, is written as

$$\frac{\partial \mathbf{u}_1}{\partial t} + \mathbf{u}_1 \frac{\partial \mathbf{u}_1}{\partial x} = \delta \left(\frac{\partial \mathbf{u}_2}{\partial t} + \mathbf{u}_2 \frac{\partial \mathbf{u}_2}{\partial x} \right) + \frac{K_{D1}}{\rho_1} \frac{\eta}{V_p^{2/3}} (\mathbf{u}_2 - \mathbf{u}_1) + \frac{K_{D2} \rho_2 S_{eff}}{\rho_1 V_p} |\mathbf{u}_2 - \mathbf{u}_1| (\mathbf{u}_2 - \mathbf{u}_1), \quad [22]$$

where $\delta = \rho_2/\rho_1$. At steady state, and with $|\mathbf{U}| = |\mathbf{u}_2 - \mathbf{u}_1| \ll \mathbf{u}_2|$, [22] becomes

$$-\mathbf{u}_2 \frac{\partial \mathbf{U}}{\partial x} = \mathbf{U} \frac{\partial \mathbf{u}_2}{\partial x} + \frac{K_{D1}}{\rho_1} \frac{\eta}{V_p^{2/3}} \mathbf{U} \quad [23]$$

or,

$$-\frac{1}{\mathbf{U}} \frac{\partial \mathbf{U}}{\partial x} = \frac{1}{\mathbf{u}_2} \frac{\partial \mathbf{u}_2}{\partial x} + \frac{K_{D1}}{\rho_1 \mathbf{u}_2} \frac{\eta}{V_p^{2/3}}. \quad [24]$$

In the absence of a gradient in $\mathbf{u}_2$, the accommodation length

$$L_U = \left| \frac{1}{\mathbf{U}} \frac{\partial \mathbf{U}}{\partial x} \right|^{-1}$$

is equal to the viscous deceleration length

$$L_D = \left| \frac{K_{D1}}{\rho_1 \mathbf{u}_2} \frac{\eta}{V_p^{2/3}} \right|^{-1},$$

as expected. Equation [24] also shows that, for a small gradient length L_{u_2} for the fluid velocity, the accommodation length can be approximately estimated as a harmonic mean of L_{u_2} and L_D, at least when the terms corresponding in [24] have the same sign. This indicates that, even in the presence of drag, we might have $\mathbf{u}_1$ different from $\mathbf{u}_2$, as long as the gradient length of $\mathbf{u}_2$ is shorter than the deceleration length L_D. This is, for example, the case at the exit of a tube, whenever the pressure is much smaller outside, in which case there is a strong acceleration of the fluid, and therefore a steep gradient in $\mathbf{u}_2$.

To illustrate this analysis, consider the following numerical application. Define the $\mathbf{u}_2$ velocity profile for $0 \leqslant x < +\infty$, such that

$$\mathbf{u}_2(x) = u_{20} + (u_{2\infty} - u_{20}) \frac{x}{x+1}. \quad [25]$$

When the boundary pressures, $P(x=0)$ and $P(x=+\infty)$ are given, we can calculate $u_{2\infty}$ through the use of Bernoulli's theorem and the equation of state $I_2 = P/(\gamma - 1)\rho_2$ for the fluid. Thus,

$$u_{2\infty} = \left\{ \frac{2\gamma}{\gamma - 1} \frac{P_0}{\rho_2} \left[1 - \left(\frac{P_\infty}{P_0} \right)^{1-\gamma/\gamma} \right] \right\}^{\frac{1}{2}}. \quad [26]$$

Pressure and density profiles are then

$$P(x) = P_0 \left[1 - \left(\frac{\gamma - 1}{2\gamma} \right) \frac{\mathbf{u}_2(x)}{u_{20}} \right]^{\frac{\gamma}{\gamma - 1}} \quad [27]$$

and

$$\rho_2(x) = \rho_0 \left(\frac{P(x)}{P_0} \right)^{\frac{1}{\gamma}}. \quad [28]$$

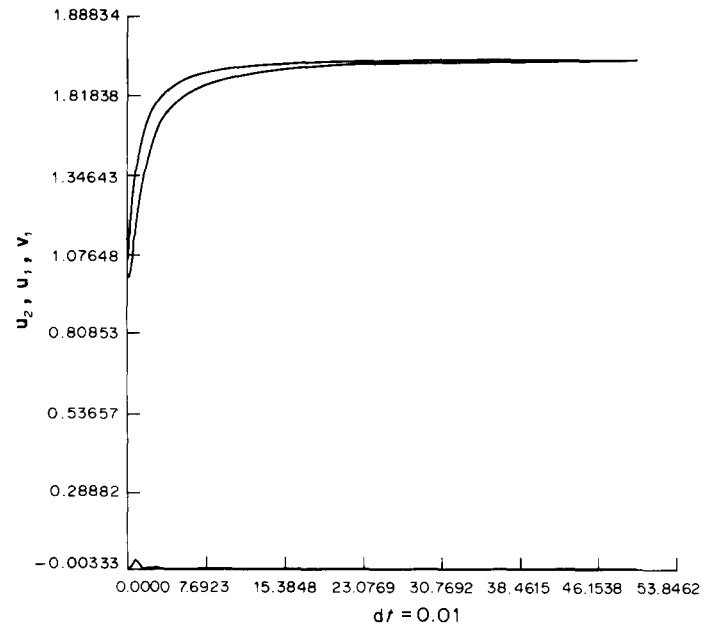

Figure 2. Behavior of a single ellipsoid in a fluid.

We solve the dimensionless version of [12] and [17]. Initially, we take $u_{10} = u_{20}$, for a particle of eccentricity $e = 0.1$, and half diameters $a = 10^{-2}$ cm, $b = 10^{-3}$ cm. The dimensionful pressures are $P = 10^7$ dyn/cm^2 and $P = 10^6$ dyn/cm^2, and u_{20} is the sound speed. Also, we take $\eta = 0.15\ 10^{-2}$ g/cm^{-1} s^{-2}, $\rho_{20} = 10^{-3}$ g/cm^{-3} and $\rho_1 = 1$ g/cm^{-3}. All Ks are of order 1 and are given this value. In figure 2, the dimensionless value of 50 for time t corresponds to the distance l_{50} for which the $\mathbf{u}_2$ profile differs by $< 1\%$ from its final value $u_{2\infty}$. In this case, the accommodation length for $\mathbf{u}_1$ is also l_{50}, which confirms [24]. In figures 3 and 4, we see that the accommodation time about the equilibrium angle $\alpha = 0$, for a vanishing angular velocity, is attained after a few oscillations. The initial angle is $-\pi/4$, and the initial angular velocity is zero.

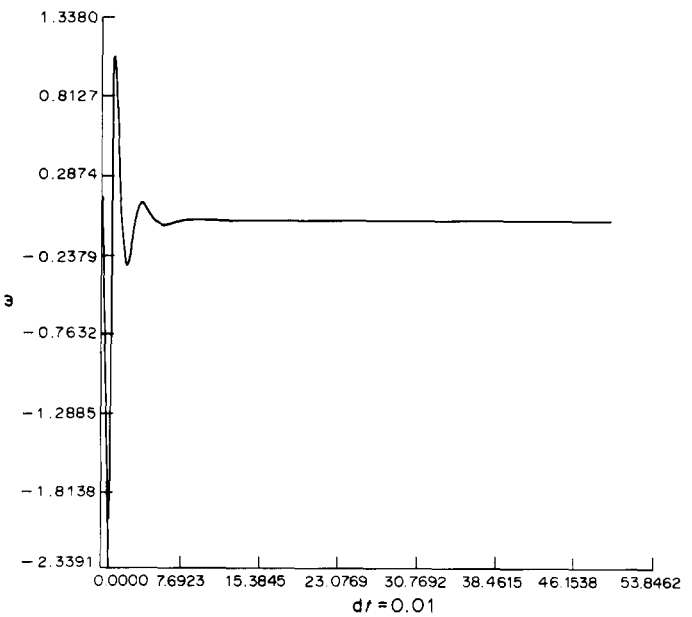

Figure 3. Behavior of a single ellipsoid in a fluid. Relaxation of the angular velocity of the particle towards zero.

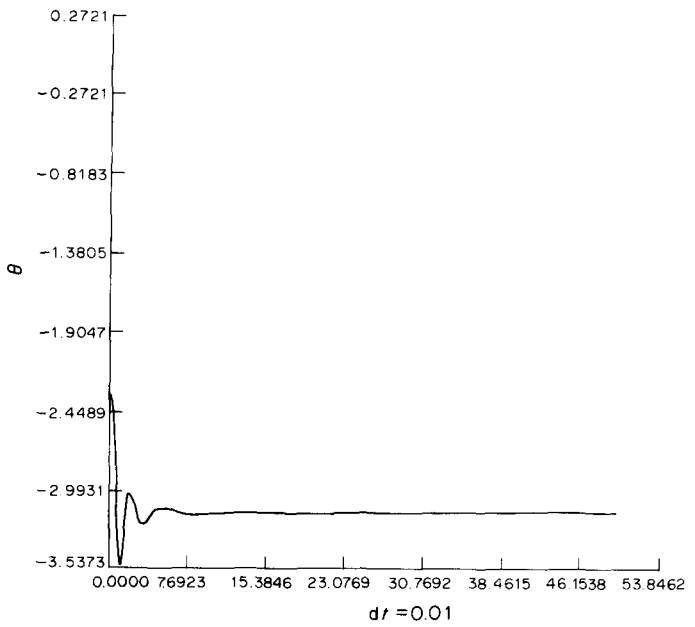

Figure 4. Behavior of a single ellipsoid in a fluid. Relaxation of the angle of the particle with the relative velocity towards zero.

3. HYBRID MODEL

3.1. Statistical description of the dispersed field

The fundamental equation for our derivation expresses the conservation of the total number of particles in an infinitesimal volume of phase space centered at position **x**, velocity **u**, angular velocity ω and orientation **n**. The central function is $N(\mathbf{x}, \mathbf{u}, \omega, \mathbf{n}, t)$, which is defined in such a way that $N\mathbf{dxdud}\omega\mathbf{dn}$ is the probable number of solid particles with position **x** within the interval **dx**, velocity **u** in **du**, angular velocity ω in $\mathbf{d}\omega$ and orientation **n** in **du**, at time t. We have

$$\frac{\partial N}{\partial t}+\frac{\partial}{\partial x_j}\left(N\frac{\mathrm{d}x_j}{\mathrm{d}t}\right)+\frac{\partial}{\partial \omega_j}\left(N\frac{\mathrm{d}u_j}{\partial t}\right)+\frac{\partial}{\partial \omega_j}\left(N\frac{\mathrm{d}\omega_j}{\partial t}\right)+\frac{\partial}{\partial u_j}\left(N\frac{\mathrm{d}u_j}{\mathrm{d}t}\right)=0, \qquad [29]$$

in which the total time derivatives are along the dynamically and kinematically allowable paths of the individual particles. Thus, if $[\mathbb{J}]$ is the tensor of inertia of the particles and F_j and T_j are the force and the torque acting on the particles.

$$\frac{\mathrm{d}x_j}{\mathrm{d}t}=u_j, \qquad [30]$$

$$m\frac{\mathrm{d}u_j}{\mathrm{d}t}=F_j, \qquad [31]$$

$$[\mathbb{J}_{ij}]\frac{\mathrm{d}\omega_i}{\mathrm{d}t}=T_j \qquad [32]$$

and

$$\frac{\mathrm{d}\mathbf{n}}{\mathrm{d}t}=\mathbf{n}\times\omega. \qquad [33]$$

We define F_j and T_j using [12] and [17]. Due to the averaging of the microscopic velocities $\mathbf{u}_2$ on the surface of the particle in these equations, we have to restrict outselves to length scales larger than the size of a particle. This also implies that the hydrodynamic scale is larger than the size of a particle. We then assume that [12] and [17] are valid for any particle

located within a given control volume over which the microscopic conservation equations for the fluid are averaged to obtain the hydrodynamics equations. This assumption implies that the Cs and Ks in [12] and [17] are proportional to the volume fraction of the fluid. This is consistent with the requirement that force per unit volume arises from the loss of available momentum, which is equal to the effective interaction area times the fraction interacting per unit time [11]. This area is assumed to be proportional to the volume fraction of the background fluid, because the fluid momentum in the control volume is proportional to the fluid volume fraction. With this restriction, our statistical model of the dispersed field is given by [29], together with [30]–[33] and [12] and [17], in which $\mathbf{u}_2$ is the fluid velocity.

Equation [29] describes the behavior of the single particle distribution function, and depends only on one-particle dynamics. Nevertheless, this equation can be considered to represent the multiparticle effects of the dispersed field through the force F_j and the torque T_j, which couple the different particles through their interactions with the surrounding fluid. A particle affects its surrounding fluid, which in turn alters the behavior of other particles located in that region of phase space.

Define

$$\rho_1' = \iiint Nm \, \mathbf{du}_1 \, d\omega \, \mathbf{dn} \tag{34}$$

and

$$\rho_1' \overline{u_{1i}} = \iiint Nmu_{1i} \, \mathbf{du}_1 \, d\omega \, \mathbf{dn}, \tag{35}$$

which are the density per unit total volume of the particles, and the mean momentum of particles located at a given point $\mathbf{x}$. If we multiply [29] by mu_{1i} and integrate it over the entire range of $\mathbf{u}_1$, ω and $\mathbf{n}$ values, we obtain

$$\frac{\delta \rho_1' \overline{u_{1i}}}{\partial t} + \frac{\partial \rho_1' \overline{u_{1i}} \overline{u_{1j}}}{\partial x_j} = -\frac{\partial}{\partial x_j} \iiint Nm \delta u_{1i} \delta u_{1j} \, du_1 \, d\omega \, \mathbf{dn} - \iiint mu_{1i} \frac{\partial}{\partial u_{1j}} \left(\frac{NF_j}{m} \right) \mathbf{du}_1 \, d\omega \, \mathbf{dn}, \tag{36}$$

in which $\delta u_{1i} = u_{1i} - \overline{u_{1i}}$. The terms in [36] can be respectively interpreted as the rate of change of total dispersed phase momentum, the contribution to momentum change from the mean convective flux, the fluctuational contribution analogous to the Reynold's stress in turbulent flow and the effect of single particle forces on the fluid momentum. This last term describes the interaction ΔI_i between the fluid and the particles at point x,

$$\Delta I_i = -\iiint mu_{1i} \frac{\partial}{\partial u_{1j}} \left(\frac{NF_j}{m} \right) \mathbf{du}_1 \, d\omega \, \mathbf{dn}. \tag{37}$$

The exchange of energy between the fluid and the particles is calculated in the same manner, except that now there are two different terms describing the exchange of kinetic and rotational energies. We obtain the kinetic energy interaction term by multiplying [29] by $\frac{1}{2} mu_{1i} u_{lj}$ and integrating the range of $\mathbf{u}_1$, ω and $\mathbf{n}$,

$$\Delta E_c = -\frac{1}{2} \iiint mu_{1i} u_{1j} \frac{\partial}{\partial u_{1j}} \left(\frac{NF_i}{m} \right) \mathbf{du}_1 \, d\omega \, \mathbf{dn}. \tag{38}$$

Multiplying [29] by $\frac{1}{2} \mathbb{J}_{il} \omega_1 \omega_l$ and integrating over the same volume gives the rotational energy interaction term,

$$\Delta E_p = -\frac{1}{2} \iiint \mathbb{J}_{il} \omega_i \omega_j \frac{\partial}{\partial \omega_j} (N \mathbb{J}_{lk}^{-1} T_k) \, \mathbf{du}_1 \, \mathbf{u}\omega \, \mathbf{dn}. \tag{39}$$

Using integration by parts, and reducing the results, we rearrange these terms as follows:

$$\Delta I_i = \iiint NF_i \, \mathbf{du}_1 \, d\omega \, \mathbf{dn}, \tag{40}$$

$$\Delta E_c = \iiint u_{1i} F_i N \mathrm{d}\mathbf{u}_1 \mathrm{d}\boldsymbol{\omega} \mathrm{d}\mathbf{n} \quad [41]$$

and

$$\Delta E_p = \iiint \mathbb{J}_{ij} \omega_i \mathbb{J}_{jl}^{-1} T_l N \, \mathrm{d}\mathbf{u}_1 \, \mathrm{d}\boldsymbol{\omega} \, \mathrm{d}\mathbf{n}. \quad [42]$$

We might also give an expression for the exchange of angular momentum between the fluid and the particles. However, because this expression does not appear in the hydrodynamical equations, one would have to derive the angular momentum conservation equation for the fluid (Travis *et al.* 1975) and this is beyond the scope of our study.

3.2. Influence of turbulence

Equation [29] expresses the conservation of the total number of particles in configuration space. It can be considered to include the effect on the particles of the fluid turbulence. In a previous study of the diffusion of spherical particles, Margolin (1977) has shown that the diffusion coefficient is, for isotropic fluid turbulence, proportional to the contraction of the Reynolds stress tensor. Equation [29] provides a powerful tool for studying the effect of turbulence on nonspherical particles.

Consider [29], which we rewrite as follows:

$$\frac{\partial N}{\partial t} + u_{1j} \frac{\partial N}{\partial x_j} + \frac{1}{m} \frac{\partial}{\partial u_{ij}} (F_j N) + \frac{\partial}{\partial \omega_j} (A_{ij} T_i N) + \frac{\partial}{\partial \xi_j} (\omega_j N) = 0, \quad [43]$$

with ξ_j and A_{ij} defined such that $\mathrm{d}\xi_j/\mathrm{d}t = \omega_j$ and $A_{il}\mathbb{J}_{lj} = \delta_{ij}$. The distribution function is separated into two parts, as are the force F_j, the torque T_j, the velocity, the fluid density and the pressure:

$$\begin{aligned} N &= \overline{N} + N', \\ F_j &= \overline{F_j} + F_j', \\ T_j &= \overline{T_j} + T_j', \\ u_{2i} &= \overline{u_{2i}} + u_{2i}', \\ \rho_2 &= \overline{\rho_2} + \rho_2' \end{aligned} \quad [44]$$

and

$$P = \overline{P} + P'.$$

The bars denote mean quantities, and the primes fluctuating quantities, such that $\overline{N'} = \overline{F_j'} = \overline{T_j'} = \overline{u_{2i}'} = \overline{P'} = \overline{\rho_2'} = 0$. Averaging [43], we obtain

$$\frac{\partial \overline{N}}{\partial t} + u_{ij} \frac{\partial \overline{N}}{\partial x_j} + \frac{1}{m} \frac{\partial}{\partial u_{ij}} (\overline{F_j N}) + \frac{\partial}{\partial \omega_j} (A_{ij} \overline{T_i N}) + \frac{\partial}{\partial \xi_j} (\omega_j \overline{N}) = -\frac{1}{m} \frac{\partial}{\partial \mu_{1j}} (\overline{F_j' N'}) - A_{ij} \frac{\partial}{\partial \omega_j} (\overline{T_i' N'}). \quad [45]$$

Subtracting [43] from [45],

$$\frac{\partial N'}{\partial t} + u_{1j} \frac{\partial N'}{\partial x_j} + \frac{1}{m} \frac{\partial}{\partial u_{1j}} (F_j' \overline{N}) + \frac{1}{m} \frac{\partial}{\partial u_{1j}} (\overline{F_j} N') + \frac{\partial}{\partial \omega_j} (A_{ij} T_i' \overline{N}) + \frac{\partial}{\partial \omega_j} (A_{ij} \overline{T_i} N') + \frac{\partial}{\partial \xi_j} (\omega_j N') - \frac{1}{m} \frac{\partial}{\partial u_{1j}} (\overline{F_j' N'}) - A_{ij} \frac{\partial}{\partial \omega_j} (\overline{T_i' N'}) = 0. \quad [46]$$

Expanding N' in powers of the turbulent fluctuating quantities F_j' and T_i' gives

$$N' = \sum_{l=1}^{+\infty} N'^{(l)}$$

with

$$N'^{(l)} = \sum_{p+q=l} B_{pqij} F_j'^{p} T_i'^{q}. \quad [47]$$

Inserting [47] into [46], we obtain an infinite system of equations, from which we keep only the first one:

$$\frac{\partial N'^{(1)}}{\partial t} + u_{1j}\frac{\partial N'^{(1)}}{\partial x_j} + \frac{1}{m}\frac{\partial}{\partial u_{1j}}(F'_j\overline{N}) + \frac{1}{m}\frac{\partial}{\partial u_{1j}}\left(\overline{F}_j N'^{(1)}\right) + \frac{\partial}{\partial \omega_j}(A_{ij}T'_i\overline{N}) + \frac{\partial}{\partial \omega_j}(A_{ij}T_i\overline{N}'^{(1)}) = 0. \quad [48]$$

We presently assume $\overline{F}_j = \overline{T}_j = 0$, since we are mostly interested in turbulence effects. We make a Fourier transformation of [48] to obtain

$$i(\omega - k_j u_{1j})N'^{(1)}_k = \int\left[\frac{\partial}{\partial u_{1j}}\left(\frac{1}{m}F'_{k_{1j}}\overline{N}_{k_2}\right) + \frac{\partial}{\partial \omega_j}\left(A_{ij}T'_{k_{1i}}\overline{N}_{k_2}\right)\right]\delta(k - k_2 - k_2)\mathrm{d}k_1\,\mathrm{d}k_2, \quad [49]$$

with $k = (k_j), j = 1,2,3$. Then combining [49] and [45], we have

$$\frac{\partial \overline{N}}{\partial t} + u_{1j}\frac{\partial \overline{N}}{\partial x_j} + \frac{\partial}{\partial \xi_j}(\omega_j\overline{N}) = -\int\overline{\left[\frac{\partial}{\partial u_{lj}}\frac{1}{m}F'_{k'_j}N'^{(1)}_k + \frac{\partial}{\partial \omega_j}\left(A_{ij}T'_{k'}N'^{(1)}_k\right)\right]}\exp[i(k_l + k'_l)x_l]\mathrm{d}k\,\mathrm{d}k' \quad [50]$$

or

$$\frac{\partial \overline{N}}{\partial t} + u_{1j}\frac{\partial \overline{N}}{\partial x_j} + \frac{\partial}{\partial \xi_j}(\omega_j\overline{N}) = i\int_{\delta\to 0+}\left\{\overline{\frac{\partial}{\partial u_{1i}}\left[\frac{F'_{k'_i}m^{-1}}{\omega - k_l u_{1l} + i\delta}\frac{\partial}{\partial u_{1j}}\left(F'_{k_{1j}}\frac{\overline{N}_{k_2}}{m}\right)\right] + \frac{\partial}{\partial \omega_i}\left[\frac{A_{li}T'_{k'_i}}{\omega - k_m u_{1m} + i\delta}\frac{\partial}{\partial \omega_j}(A_{ij}T'_{k'}\overline{N'_{k_2}})\right]}\right\} \times \exp[i(k_l + k'_l)x_l]\delta(k - k_1 - k_2)\mathrm{d}k_1\,\mathrm{d}k_2\,\mathrm{d}k\,\mathrm{d}k'. \quad [51]$$

This equation shows the quasilinear approximation for turbulence effects on the distribution function $\overline{N}$.

More details can be given in the case of a small relative velocity between the two fields. Equations [12] and [17] can be rewritten as follows:

$$\frac{\mathbf{F}}{m} = -\frac{1}{\rho_1}\nabla P + \eta V_p^{1/3}\frac{K_{D1}}{\rho_1}(\mathbf{u}_2 - \mathbf{u}_1) + \frac{C_{L1}}{\rho_1}\left(\mathbf{n}\times\frac{\mathbf{u}_2 - \mathbf{u}_1}{|\mathbf{u}_2 - \mathbf{u}_1|}\right)(\mathbf{u}_2 - \mathbf{u}_1)\{-\mathrm{sign}[\mathbf{n}\cdot(\mathbf{u}_2 - \mathbf{u}_1)]\}, \quad [52]$$

and

$$\mathbf{T} = K_{\omega 1}\eta V_p(\tfrac{1}{2}\nabla\times\mathbf{u}_2 - \omega) - K_{\omega 3}\eta b(a-b)\left[\left(\mathbf{n}\cdot\frac{\mathbf{u}_2 - \mathbf{u}_1}{|\mathbf{u}_2 - \mathbf{u}_1|}\right)[\mathbf{n}\times(\mathbf{u}_2 - \mathbf{u}_1)]\right]. \quad [53]$$

The condition $\overline{\mathbf{F}} = \overline{\mathbf{T}} = 0$ is fulfilled when $\nabla\cdot P = 0$ and $\mathbf{u}_1 = \overline{\mathbf{u}_2}$ (i.e. the particles are accommodated to the surrounding fluid). Thus,

$$\frac{\mathbf{F}}{\mathbf{m}} = -\frac{1}{\rho_1}\nabla P' + \eta V_p^{1/3}\frac{K_{D1}}{\rho}\mathbf{u}'_1 + \frac{C_{L1}}{\rho_1}\left(\mathbf{n}\times\frac{\mathbf{u}'_2}{|\mathbf{u}'_1|}\right)\times\mathbf{u}'_1 \quad [54]$$

and

$$\mathbf{T}' = K_{\omega 1}\eta V_{p\frac{1}{2}}\nabla\times\mathbf{u}'_2 - K_{\omega 3}\eta b(a-b)\left(\mathbf{n}\cdot\frac{\mathbf{u}'_2}{|\mathbf{u}'_2|}\right)(\mathbf{n}\times\mathbf{u}'_2). \quad [55]$$

The turbulent fluctuating force $\mathbf{F}'$ and torque $\mathbf{T}'$ do not depend on $\mathbf{u}_1$ and ω, so [51] becomes

$$\frac{\partial \overline{N}}{\partial t} + u_{1j}\frac{\partial \overline{N}}{\partial x_j} + \omega_j\frac{\partial \overline{N}}{\partial \xi_j} = i\int_{\delta\to 0+}\left[\frac{1}{m^2}\overline{F'_{k'_i}F'_{k_{1j}}}\frac{\partial}{\partial u_{1i}}\left(\frac{1}{\omega - k_l u_{1l} + i\delta}\frac{\partial \overline{N}_{k_2}}{\partial u_{1j}}\right)\right.$$

$$+ A_{li}A_{nj}\overline{T'_{k_l}T'_{k_{1n}}}\frac{\partial}{\partial\omega_i}\left(\frac{1}{\omega - k_l u_{1l} + i\delta}\frac{\delta\overline{N_{k_2}}}{\partial\omega_j}\right)\Bigg]$$

$$\times \exp[i(k_l + k'_l)x_l]\delta(k - k_1 - k_2)\mathrm{d}k_1\mathrm{d}k_2\mathrm{d}k\mathrm{d}k'. \qquad [56]$$

Assuming that $\overline{N}$ changes much more slowly than the turbulent field [i.e. $\overline{N_{k_2}} = \overline{N}\delta(k_2)$], we transform [56] in to

$$\frac{\partial\overline{N}}{\partial t} + u_{1j}\frac{\partial\overline{N}}{\partial x_j} + \omega_j\frac{\partial\overline{N}}{\partial\xi_j} = i\left\{\frac{\partial}{\partial u_{1i}}\left[\int\frac{1}{m^2}\overline{F'_{k_i}F'_{k_j}}\frac{\exp[i(k'_l + k'_l)x_l]}{\omega - k_l u_{1l} + iv}\,\mathrm{d}k\mathrm{d}k'\right]\frac{\partial\overline{N}}{\partial u_{1j}}\right.$$

$$\left. + \frac{\partial}{\partial\omega_i}\left[\int A_{li}A_{nj}\overline{T'_{k_l}T'_{k_{1n}}}\frac{\exp[i(k'_l + k'_l)x_l]}{\omega - k_l u_{1l} + i\delta}\,\mathrm{d}k\mathrm{d}k'\right]\frac{\partial\overline{N}}{\partial\omega_j}\right\}. \qquad [57]$$

Equation [57] shows that the introduction of turbulence leads to two diffusional effects in phase space, the diffusion coefficient for velocity U_{ij} and angular velocity W_{ij} being given by

$$U_{ij} = i\int_{\delta\to 0}\frac{1}{m^2}\overline{F'_{k_i}F'_{k_j}}\frac{\exp[i(k'_l + k'_l)x_l]}{\omega - k_l u_{1l} + i\delta}\,\mathrm{d}k\mathrm{d}k' \qquad [58]$$

and

$$W_{ij} = i\int_{\delta\to 0}A_{li}A_{nj}\overline{T'_{k_l}T'_{k_{1n}}}\frac{\exp[i(k'_l + k'_l)x_l}{\omega - k_l u_{1l} + i\delta}\,\mathrm{d}k\mathrm{d}k'. \qquad [59]$$

If we neglect the pressure fluctuations, we have, for spherical particles

$$\overline{F'_i F'_j} = (k_{\mathrm{D1}}\eta V_\rho^{2/3})\overline{u'_{2i}u'_{2j}}, \qquad [60]$$

which is nothing other than the Reynolds stress tensor of the surrounding fluid. This clearly shows the dependence of U_{ij} and W_{ij} on the fluid turbulence variables.

The form of the diffusion coefficients in [58] and [59] indicates the interaction between each spectral component of the fluid turbulence with the particles. Another approach for describing turbulence would be to relate the fluctuating part of the distribution function N to spectrum-integrated turbulent variables (e.g. the Reynolds stress tensor), in order to couple the transformed [57] to turbulence models such as in Besnard & Harlow (1985) and Daly & Harlow (1970). Such a model will be presented in a subsequent paper.

3.3. Dimensionless equations

The dispersed phase is described by [29], together with [12] and [17]. We now consider the fluid equations:

$$\frac{\partial\rho_2\alpha_2}{\partial t} + \frac{\partial\rho_2\alpha_2 u_{2j}}{\partial x_j} = 0, \qquad [61]$$

$$\frac{\partial\rho_2\alpha_2 u_{2i}}{\partial t} + \frac{\partial\rho_2\alpha_2 u_{2i}u_{2j}}{\partial x_j} = -\alpha_2\frac{\partial P}{\partial x_i} - \Delta I_i \qquad [62]$$

and

$$\frac{\partial\rho_2\alpha_2 E_2}{\partial t} + \frac{\partial\rho_2\alpha_2 u_{2j}E_2}{\partial x_j} = -\frac{\partial\alpha_2 u_{2j}P}{\delta x_j} - P\frac{\partial\alpha_2}{\partial t} - \Delta E_{\mathrm{c}} - \Delta E_{\mathrm{p}}, \qquad [63]$$

with ΔI_{i}, ΔE_{c} and ΔE_{p} given by [40]–[42]. In [63], E_2 denotes the total energy per unit volume of the fluid.

We define the dimensionless variables $\hat{\mathbf{u}}_2$, $\hat{\rho}_2$, $\hat{t}$, $\hat{x}_i$, $\hat{P}$, $\hat{\boldsymbol{\omega}}$, $\hat{E}_2$, $\hat{\mathbf{u}}_2$, and the dimensionful constants U, ρ_2^0, x_0, such that $\hat{\mathbf{u}}_2 = \mathbf{u}_2/U$, $\hat{\rho}_2 = \rho_2^0\rho_2$, $t = \hat{t}x_0/U$, $\hat{x}_j = x_j/x_0$, $\hat{P} = P/\rho_2^0 U^2$, $\hat{\boldsymbol{\omega}} = \boldsymbol{\omega}x_o/U$, $\hat{E}_2 = E_2/U^2$ and $u_{1j} = u_{1j}/U$. With these definitions, the model equations

[29]–[33] and [61]–[63] become

$$\frac{\partial N}{\partial \hat{t}} + \frac{\partial}{\partial \hat{x}_j}\left(N\frac{\mathrm{d}\hat{x}_i}{\mathrm{d}t}\right) + \frac{\partial}{\partial \alpha_j}\left(N\frac{\mathrm{d}\alpha_j}{\mathrm{d}t}\right) + \frac{\partial}{\partial \hat{\omega}_j}\left(N\frac{\mathrm{d}\hat{u}_j}{\mathrm{d}\hat{t}}\right) + \frac{\partial}{\partial \hat{u}_{1j}}\left(N\frac{\mathrm{d}\hat{u}_{1j}}{\mathrm{d}t}\right) = 0, \quad [64]$$

$$\frac{\mathrm{d}\hat{x}_j}{\mathrm{d}\hat{t}} = \hat{u}_{1j}, \quad [65]$$

$$\frac{\mathrm{d}\alpha_j}{\mathrm{d}\hat{t}} = \hat{\omega}_i, \quad [66]$$

$$\mathbb{J}: \frac{\mathrm{d}\hat{\boldsymbol{\omega}}}{\mathrm{d}\hat{t}} = \frac{x_0}{U}K_{\omega 1}\eta V_\mathrm{p}(\tfrac{1}{2}\hat{\nabla}\times\hat{\mathbf{u}}_2 - \hat{\boldsymbol{\omega}}) + \tfrac{1}{2}K_{\omega 2}\hat{\rho}_2\rho_2^0 a(a-b)S_\mathrm{p}\mathrm{A}(\beta)|\hat{\mathbf{u}}_2 - \hat{\mathbf{u}}_1|(\tfrac{1}{2}\hat{\nabla}\times\hat{\mathbf{u}}_2 - \hat{\boldsymbol{\omega}}) - \frac{x_0}{U}K_{\omega 3}\eta b(a-b)\mathbf{n}\cdot\frac{\hat{\mathbf{u}}_2 - \hat{\mathbf{u}}_1}{|\hat{\mathbf{u}}_2 - \hat{\mathbf{u}}_1|}[\mathbf{n}\times(\hat{\mathbf{u}}_2 - \hat{\mathbf{u}}_1)] + \tfrac{1}{2}K_{\omega 4}\hat{\rho}_2\rho_2^0(a-b)S_\mathrm{p}[\mathbf{n}\cdot(\hat{\mathbf{u}}_2 - \hat{\mathbf{u}}_1)][\mathbf{n}\times(\hat{\mathbf{u}}_2 - \hat{\mathbf{u}}_1)], \quad [67]$$

$$\beta = (\mathbf{n}, \hat{\mathbf{u}}_2 - \hat{\mathbf{u}}_1),$$

$$m\frac{\mathrm{d}\hat{\mathbf{u}}_1}{\mathrm{d}\hat{t}} = -\rho_2^0 V_\mathrm{p}\hat{\nabla}\hat{P} + \frac{x_0}{U}K_{\mathrm{D}1}\eta V_\mathrm{p}^{1/3}(\hat{\mathbf{u}}_2 - \hat{\mathbf{u}}_1) + K_{\mathrm{D}2}\rho_2 x_0 S_\mathrm{eff}|\hat{\mathbf{u}}_2 - \hat{\mathbf{u}}_1|(\hat{\mathbf{u}}_2 - \hat{\mathbf{u}}_1) + \frac{x_0}{U}C_{\mathrm{L}1}\left(\mathbf{n}\times\frac{\hat{\mathbf{u}}_2 - \hat{\mathbf{u}}_1}{|\hat{\mathbf{u}}_2 - \hat{\mathbf{u}}_1|}\right)\times(\hat{\mathbf{u}}_2 - \hat{\mathbf{u}}_1)\{-\mathrm{sign}[\mathbf{n}\cdot(\hat{\mathbf{u}}_2 - \hat{\mathbf{u}}_1)]\} + x_0 C_{\mathrm{L}2}[\mathbf{n}\times(\hat{\mathbf{u}}_2 - \hat{\mathbf{u}}_1)]\times(\hat{\mathbf{u}}_2 - \hat{\mathbf{u}}_1)\{-\mathrm{sign}[\mathbf{n}\cdot(\hat{\mathbf{u}}_2 - \hat{\mathbf{u}}_1)]\}, \quad [68]$$

$$\frac{\partial \alpha_2\hat{\rho}_2}{\partial \hat{t}} + \frac{\partial \alpha_2\hat{\rho}_2\hat{u}_{2j}}{\partial \hat{x}_j} = 0, \quad [69]$$

$$\frac{\partial \alpha_2\hat{\rho}_2\hat{u}_{2i}}{\partial \hat{t}} + \frac{\partial \alpha_2\hat{\rho}_2\hat{u}_{2i}\hat{u}_{2j}}{\partial x_j} = -\alpha_2\frac{\partial \hat{P}}{\partial \hat{x}_i} - \Delta\hat{I}_i \quad [70]$$

and

$$\frac{\partial \alpha_2\hat{\rho}_2\hat{E}_2}{\partial \hat{t}} + \frac{\partial \alpha_2\hat{\rho}_2\hat{u}_{2j}\hat{E}_2}{\partial \hat{x}_j} = -\frac{\partial \alpha_2\hat{u}_{2j}\hat{P}}{\partial \hat{x}_j} - \hat{P}\frac{\partial \alpha_2}{\partial \hat{t}} - \Delta\hat{E}_\mathrm{c} - \Delta\hat{E}_\mathrm{p}, \quad [71]$$

where

$$\Delta\hat{I}_i = \frac{x_0}{\rho_2^0 U^2}\Delta I_i,\ \Delta\hat{E}_\mathrm{c} = \frac{x_0}{U^3\rho_2^0}\Delta E_\mathrm{c} \quad \text{and} \quad \Delta E_\mathrm{p} = \frac{x_0}{U^3\rho_2^0}\Delta E_\mathrm{p}.$$

4. NUMERICAL APPLICATIONS

4.1. Application to 2-D plane geometry

To illustrate the possibilities of this model, a code has been written to solve the system of equations [64]–[71] for stationary flows in 2-D plane geometry. We have examined two-field flows consisting of a high-speed jet of fluid with entrained ellipsoidal particles escaping from a tube. Preliminary numerical studies showed that the effect of the fluid vorticity is negligible in this special case. We thus specialize [64]–[71] to 2-D plane geometry, with the particle velocity components u_{1x} and u_{1y}, and the fluid velocity components u_{2x} and u_{2y} located on the axes x and y, respectively. The angular velocity has only one non-zero component along the z-axis. Omitting the $\hat{}$ sign above the variables, we obtain

$$\frac{\partial \omega}{\partial t} + \frac{\partial}{\partial x}\left(N\frac{\mathrm{d}x}{\mathrm{d}t}\right) + \frac{\partial}{\partial y}\left(N\frac{\mathrm{d}y}{\mathrm{d}t}\right) + \frac{\partial}{\partial \omega}\left(N\frac{\mathrm{d}\omega}{\mathrm{d}t}\right) + \frac{\partial}{\partial \xi}\left(N\frac{\mathrm{d}\xi}{\mathrm{d}t}\right) + \frac{\partial}{\partial u_{1x}}\left(N\frac{\mathrm{d}u_{1x}}{\mathrm{d}t}\right) + \frac{\partial}{\partial u_{1y}}\left(N\frac{\mathrm{d}u_{1y}}{\mathrm{d}t}\right) = 0, \quad [72]$$

$$\frac{dx}{dt} = u_{1x}, \tag{73}$$

$$\frac{dy}{dt} = u_{1y}, \tag{74}$$

$$\frac{d\xi}{dt} = \omega, \tag{75}$$

$$\begin{aligned}\frac{d\omega}{dt} = &-\frac{x_0}{U}\mathbb{J}^{-1}K_{\omega 1}V_p\omega - \frac{\mathbb{J}^{-1}}{2}K_{\omega 2}\rho_2^0\rho_2 a(a-b)S_p A(\beta)[(u_{2x}-u_{1x})^2 \\ &+ (u_{2y}-u_{1y})^2]^{1/2}\omega + \left\{-\mathbb{J}^{-1}\frac{x_0}{U}K_{\omega 3}\eta b(a-b)[(u_{2x}-u_{1x})^2\right. \\ &\left.+ (u_{2y}-u_{1y})^2] + \frac{\mathbb{J}^{-1}}{2}K_{\omega 4}\rho_2^0\rho_2(a-b)S_p\right\}[(u_{2x}-u_{1x})\sin\xi \\ &- (u_{2y}-u_{1y})\cos\xi][(u_{2x}-u_{1x})\cos\xi + (u_{2y}-u_{1y})\sin\xi],\end{aligned} \tag{76}$$

$$\begin{aligned}\frac{du_{1x}}{dt} = &-\frac{\rho_2^0}{\rho_1}\frac{\partial P}{\partial x} + \frac{x_0}{U}\frac{\eta}{\rho_1 V_p^{2/3}}K_{D1}(u_{2x}-u_{1x}) \\ &+ \frac{x_0\rho_2 S_{\text{eff}}}{\rho_1 V_p}K_{D2}[(u_{2x}-u_{1x})^2 + (u_{2y}-u_{1y})^2]^{1/2}(u_{2x}-u_{1x}) \\ &- \delta\left\{\frac{x_0}{U}\frac{C_{L1}}{\rho_1 V_p}[(u_{2x}-u_{1x})^2 + (u_{2y}-u_{1y})^2]^{-1/2}\right. \\ &\left.+ \frac{C_{L2}}{\rho_1 V_p}\right\}(u_{2y}-u_{1y})[(u_{2y}-u_{1y})\cos\xi - (u_{2x}-u_{1x})\sin\xi]\end{aligned} \tag{77}$$

and

$$\begin{aligned}\frac{\partial u_{1y}}{dt} = &-\frac{\rho_2^0}{\rho_1}\frac{\delta P}{\partial y} + \frac{x_0}{U}\frac{\eta}{\rho_1 V_p^{2/3}}K_{D1}(u_{2y}-u_{1y}) + \frac{x_0\rho_2 S_{\text{eff}}}{\rho_1 V_p}K_{D2}[(u_{2x}-u_{1x})^2 \\ &+ (u_{2y}-u_{1y})^2]^{1/2}(u_{2y}-u_{1y}) - \delta\left\{\frac{x_0}{U}\frac{C_{L1}}{\rho_1 V_p}[(u_{2x}-u_{1x})^2\right. \\ &\left.+ (u_{2y}-u_{1y})^2]^{-1/2} + \frac{C_{L2}}{\rho_1 V_p}\right\}(u_{2x}-u_{2x})[(u_{2y}-u_{1y})\cos\xi \\ &- (u_{2x}-u_{1x})\sin\xi],\end{aligned} \tag{78}$$

with $\delta = \text{sign}[\mathbf{n}\cdot(\mathbf{u}_2 - \mathbf{u}_1)]$,

$$\frac{\partial\alpha_2\rho_2}{\partial t} + \frac{\partial\alpha_2\rho_2 u_{2x}}{\partial x} + \frac{\partial\alpha_2\rho_2 u_{2y}}{\partial y} = 0. \tag{79}$$

$$\frac{\partial\alpha_2\rho_2 u_{2x}}{\partial t} + \frac{\partial\alpha_2\rho_2 u_{2x}^2}{\partial x} + \frac{\partial\alpha_2\rho_2 u_{2x}u_{2y}}{\partial y} = -\alpha_2\frac{\partial P}{\partial x} - \Delta I_x, \tag{80}$$

$$\frac{\partial\alpha_2\rho_2 u_{2y}}{\partial t} + \frac{\partial\alpha_2\rho_2 u_{2x}u_{2y}}{\partial x} + \frac{\partial\alpha_2\rho_2 u_{2y}^2}{\partial y} = -\alpha_2\frac{\partial P}{\partial y} - \Delta I_y \tag{81}$$

and

$$\frac{\partial\alpha_2\rho_2 E_2}{\partial t} + \frac{\partial\alpha_2\rho_2 u_{2x}E_2}{\partial x} + \frac{\partial\alpha_2\rho_2 u_{2y}E_2}{\partial y} = -\frac{\delta\alpha_2 u_{2x}P}{\partial x} - \frac{\partial\alpha_2 u_{2y}P}{\partial y} - P\frac{\partial\alpha_2}{\partial t} - \Delta E_c - \Delta E_p. \tag{82}$$

We assume that the equation of state of the gas is

$$E_2 = P/(\gamma - 1)\rho_2. \tag{83}$$

In [77] and [78], C_{L1} and C_{L2} are given by [9] and [11], where [11] shows that C_{L2} is proportional to $(\sin^2\beta|B(\beta))$. With this precision, all the dependencies in the different variables are given explicitly in [72]–[83].

4.2. Numerical scheme

The Liouville equation [72] is solved in conjunction with a particle method; that is, the distribution function N is approximated by a sum of weighted Dirac δ-functions, corresponding to test particles that are followed along their trajectories. The interaction between each test particle and the surrounding fluid is calculated cell by cell along these trajectories, defined by [73]–[78]. The fluid equations [79]–[83] are solved using the particle-in-cell method, as in Travis *et al.* (1975), in which shocks are smoothed out by artificial viscosity. These two techniques are coupled in the following manner. First, assume that $\alpha_1 = 0$ and solve the fluid equations for ρ_2, u_{2x}, u_{2y} and P until steady state is achieved. Then, solve for the particle trajectories, holding the fluid variables constant, to obtain the cell-averaged particles variables α_1, u_{1x}, u_{1y}, ξ and ω. Finally, set $\alpha_2 \equiv 1 - \alpha_1$ and use the averaged particle variable values in the fluid–particle interaction terms to solve for p_2, u_{2x}, u_{2y} and P by iteration until steady state is reached. After calculation of the test particle trajectories, we can deduce the cell-averaged volume fractions and velocities for the particles. This is done by assuming that the particle momentum of a given cell is the sum of the momenta of the particles located within the cell.

Defining α_{1n} as the volume fraction of particles in the tube, and n_{1n} as the number of test particles created in a given input cell, than $\alpha_1 = \alpha_{1n} n / n_{1n}$, where n is the number of particles presently in the cell. We then assume that [12] and [17] are valid when $\mathbf{u}_1$ is replaced by $\mathbf{u}_{1\,\mathrm{av}}$, the cell-averaged velocity, calculated from the velocities of the particles located in the cell. After the advection of the fluid variables, we use a semi-implicit scheme for the Lagrangian phase of the calculation (implicit for the coupling terms), which provides stability even for strong coupling between the particles and the fluid. Equation [77] is discretized as follows:

$$\begin{aligned}\frac{u_{1x}^{n+1} - u_{1x}^{n}}{\mathrm{d}t} = \Bigg[\Bigg(-\frac{\rho_2^0}{\rho_1}\frac{\delta P^n}{\partial x}\Bigg) + \frac{x_0}{U}\frac{\eta}{\rho_1 V_\rho^{\frac{4}{3}}} K_{\mathrm{D1}}(u_{2x}^{n+1} - u_{1x}^{n+\frac{1}{2}}) \\ + K_{\mathrm{D2}}\frac{x_0 \rho_2 S_{\mathrm{eff}}}{\rho_1 V_{\mathrm{p}}}[(u_{2x}^{n} - u_{1x}^{n+\frac{1}{2}})^2 \\ + (u_{2y}^{n} - u_{1y}^{n+\frac{1}{2}})^2]^{\frac{1}{2}}(u_{2x}^{n+1} - u_{1x}^{n+\frac{1}{2}}) \\ - \delta^n \Bigg\{\frac{x_0}{U}\frac{C_{\mathrm{L1}}}{\rho_1 V_{\mathrm{p}}}[(u_{2x}^{n} - u_{1x}^{n+\frac{1}{2}})^2 + (u_{2y}^{n} - u_{1y}^{n+\frac{1}{2}})^2]^{-\frac{1}{2}} \\ + \frac{C_{\mathrm{L2}}}{\rho_1 V_{\mathrm{p}}}\Bigg\}[(u_{2y}^{n} - u_{1y}^{n+\frac{1}{2}})\cos\xi^n \\ - (u_{2x}^{n} - u_{1x}^{n+\frac{1}{2}})\sin\xi^n](u_{2y}^{n} - u_{1y}^{n+\frac{1}{2}})\Bigg],\end{aligned} \tag{84}$$

A similar discretization is used for [78]. The energy equation is then solved, with the source of energy ΔE_{c} taken equal to

$$\Delta E_{\mathrm{c}} = \frac{\rho_2^0 \rho_2}{\rho}\left[\frac{\mathrm{d}u_{1x}^{n+\frac{1}{2}}}{\mathrm{d}t}(u_{2x}^{n} - u_{1x}^{n+\frac{1}{2}}) + \frac{\mathrm{d}u_{2y}^{n+\frac{1}{2}}}{\mathrm{d}t}(u_{2y}^{n} - u_{1y}^{n+\frac{1}{2}})\right]. \tag{85}$$

In this study, ΔE_{p} is neglected. The location of the variables is shown in figure 5.

4.3. Numerical results

We present results for the case of a high-speed gas jet with entrained ellipsoidal particles, impinging in a rectangular obstacle, as shown in figure 6. The sonic two-fluid flow in the pipe expands at the exit to fill the cavity, and, after impinging on the rectangular obstacle, to exit through the open region above the obstacle. The input pressure is 10^6 dyn/cm^2, and the other dimensionful quantities are $y_0 = 1$ cm, $\rho_1 = 1$ g/cm^{-3}, $\rho_2 = 10^{-3}$ g/cm^{-3}, $U = 3.3\ 10^4$ cm s^{-1}. The length x_0 corresponds to the radius of the pipe. We choose $x_{\mathrm{obs}} = 5$, $y_{\mathrm{obs}} = 8$, $x_l = 32$, $y_l = 15$ and $x_1 = 5$.

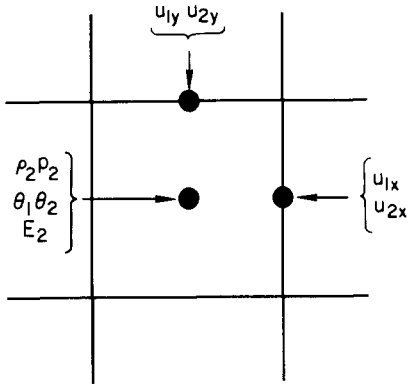

Figure 5. Location of the discretized variables on a cell of the mesh.

The first calculation considered spherical particles ($a = b = 10^{-4}$ cm), with $\alpha_1 = 10^{-4}$ at the exit of the pipe.

Figures 7a–d display the steady-state patterns simulating the circumstances described above. They are, respectively, the density and pressure contours and particle and fluid velocity fields. Figures 7a,b show an expansion of the jet at the exit of the pipe, a shock at the obstacle (which is smeared out due to the artificial viscosity and the coarseness of the grid), a discontinuity in the fluid flow at the obstacle due to the gas inside the cavity. Particles are not lifted but are partially deposited by the flow in the region of the obstacle. This is also indicated in figure 8a, which shows that the concentration of particles increases in the region of the obstacle. In this model we assume that, when particles hit the obstacle, they stick to the wall, and we neglect the effect of their accumulation. The effect of the particles size is shown by comparing figures 8a,c with figures 8b,d, where the same results are displayed for $a = 10^{-4}$ and $a = 10^{-3}$. In the last case, particle inertia exceeds the drag effect and most of the particles impact on the obstacle.

We now consider ellipsoidal particles of equivalent radius $a = 10^{-3}$, and eccentricity $e = 0.5$. The equivalent radius of a particle is the radius of a spherical particle of same mass. Figures 9a–d show plots of the particle volume fraction and velocity as well as the angular velocity and orientation of the particles. In figure 9d, all of the particles have the same orientation at the exit of the pipe, but they gradually rotate in the cavity due to the fluid torque. The length scale of the rotation can be compared with the relaxation lengths calculated in section 2.

For the same equivalent radius of 10^{-3} cm (i.e. same weight), figures 10a–d show results for a different eccentricity. The initial orientation is the same as in the previous run. Other runs with different initial orientations, not presented here, have shown that the qualitative result of figure 10d is not changed. Figures 10a–d show clearly that a diminution of particle

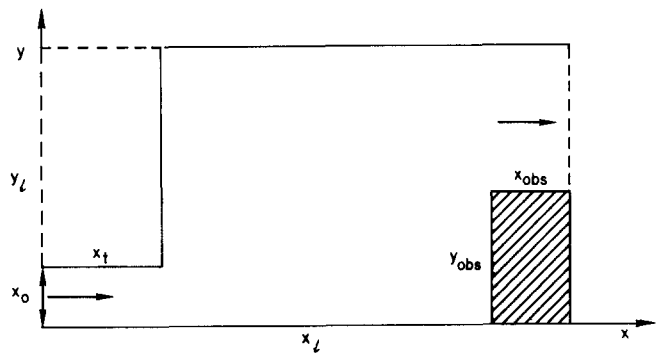

Figure 6. Spatial configuration of the test problem.

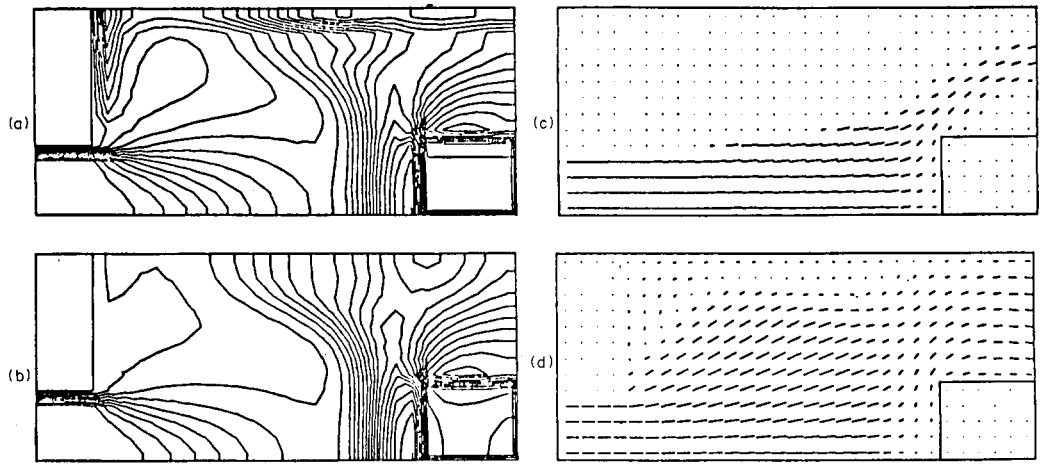

Figure 7. Steady-state patterns: $U = 3.3 \times 10^4$, $\rho_0 = 1 \times 10^6$, $\rho_1 = 1$, $\rho_2 = 1 \times 10^{-3}$, $\alpha_1 = 10^{-4}$, $a = 10^{-4}$, $b = a$. (a) Fluid density; (b) fluid pressure; (c) particles' velocity; (d) fluid velocity.

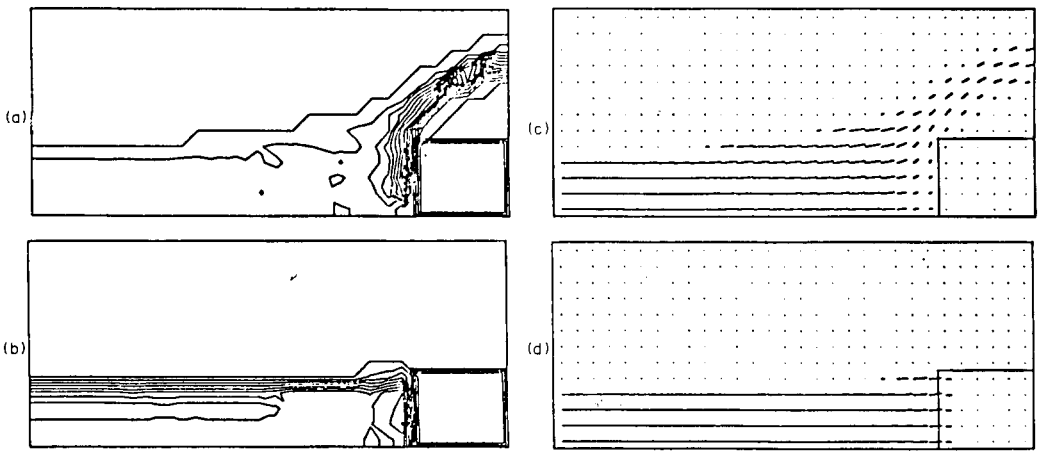

Figure 8. Steady-state patterns: (a) particles' volume fraction ($a = 10^{-4}$); (b) particles' volume fraction ($a = 10^{-3}$); (c) particles' velocity ($a = 10^{-4}$); (d) particles' velocity ($a = 10^{-3}$).

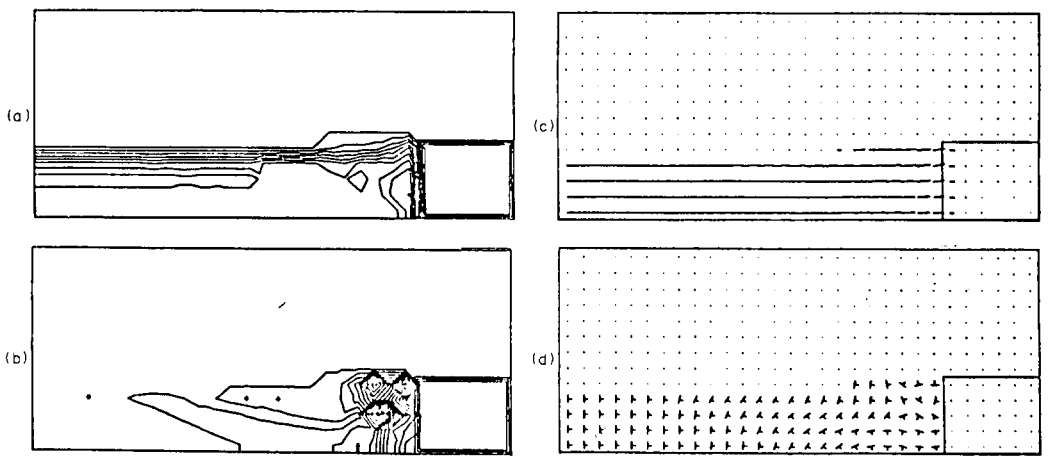

Figure 9. Steady-state patterns: $a = 2^{1/3} \times 10^{-3}$, $a_{eq} = 10^{-3}$, $m_p/m_f = 1$, $e = 0.5$. (a) Particles' volume function; (b) angular velocity; (c) particles' velocity; (d) particles' orientation.

eccentricity, i.e. an increased flatness of the particle, induces a greater sensitivity to lift and torque. Rotation takes place immediately after the exit from the pipe, and the particle orientation more closely follows the fluid stream lines (i.e. in the vicinity of the obstacle, their rotation is more important). We also notice that some particles flow past the obstacle, although most of the particles impact on the obstacle, due to their large inertia. The particles penetrate the stagnation region, the pressure gradient being too small to prevent their penetration in this region. Figure 10d also shows that the length scale of oscillation is much shorter than is the preceeding cases.

Results are displayed in figures 11a–d for the case $e = 0.01$, the other parameters being kept at the values in figures 10a–d. The trends shown in the previous points are clearer here. Oscillations of the particles are visible (note that the angular velocity changes sign in figure 11b), and we also see a shorter accommodation time in figure 11d, where the particles tend to be aligned perpendicular to the fluid velocity vector.

In figures 12a–d we consider the extreme case $e = 0.001$, when particles can be considered as disks. Their sensitivity to lift and rotation is illustrated by figure 12c. Even at the exist of the pipe, particles are lifted and follow the trajectories determined by the fluid velocity vectors everywhere except in the recirculation region. They accommodate to the flow almost immediately, oscillating around their equilibrium orientation. Another

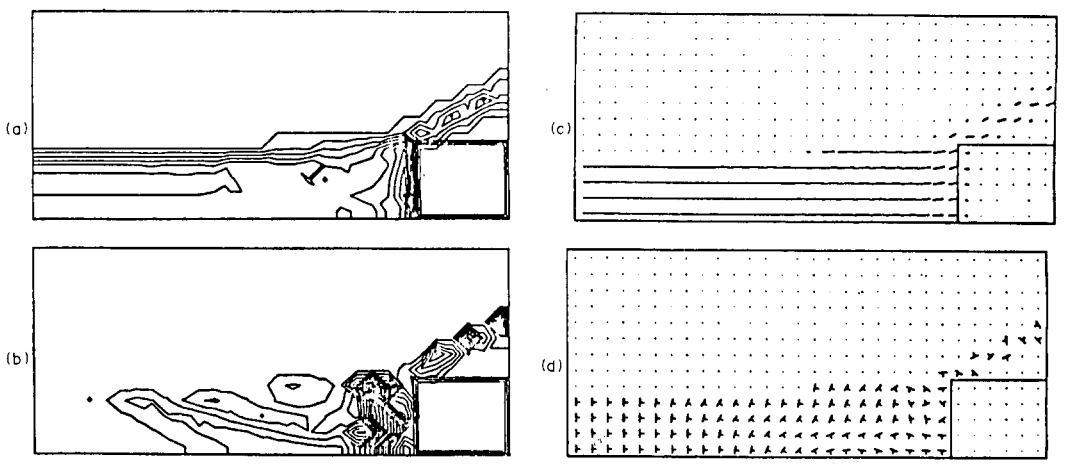

Figure 10. Steady-state patterns: $a = 5^{1/3} \times 10^{-3}$, $a_{eq} = 10^{-3}$, $e = 0.2$. (a) Particles' volume fraction; (b) angular velocity; (c) particles' velocity; (d) particles' orientation.

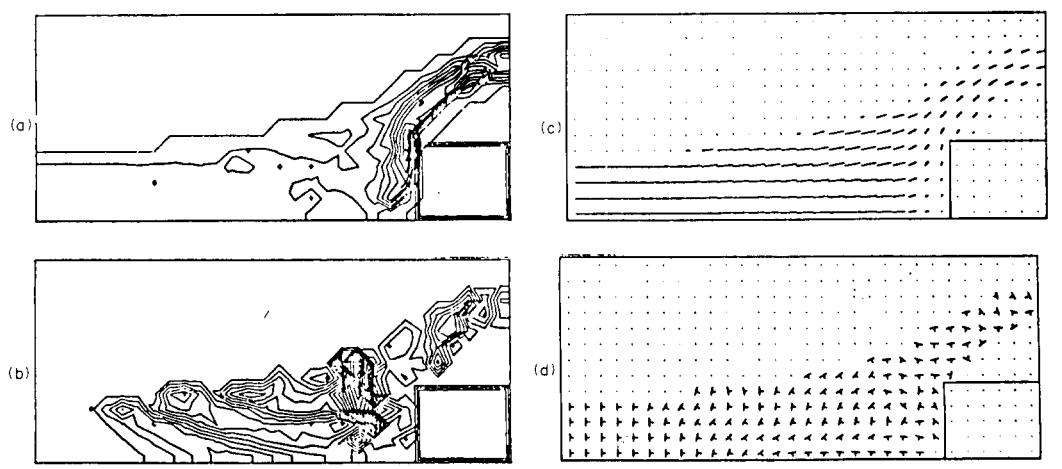

Figure 11. Steady-state patterns: $a = 10^{2/3} \times 10^{-3}$, $a_{eq} = 10^{-3}$, $e = 0.01$. (a) Particles' volume fraction; (b) angular velocity; (c) particles' velocity; (d) particles' orientation.

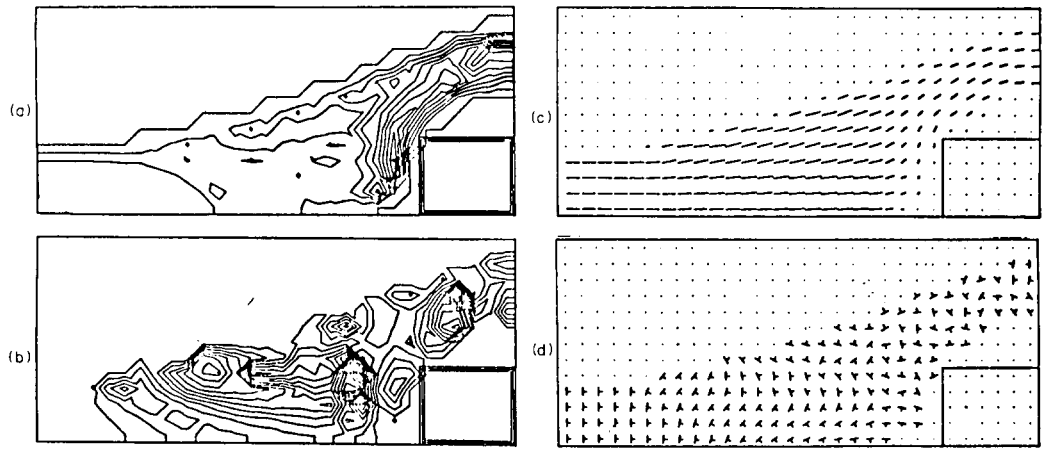

Figure 12. Steady-state patterns: $a = 10^{-2}$, $a_{eq} = 10^{-3}$, $e = 0.001$. (a) Particles' volume fraction; (b) angular velocity; (c) particles' velocity; (d) particles' orientation.

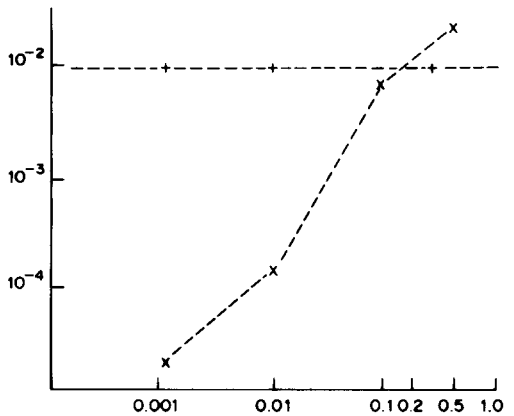

Figure 13. Forced exerted on the obstacle vs eccentricity of the particles: +, due to the fluid ($\times 10^{-1}$); ×, due to the particles.

interesting feature is that particles do not penetrate the stagnation region and, therefore, do not impact on the obstacle. This illustrates the strong influence of the particles' eccentricity on the force exerted on the obstacle.

Figure 13 shows a plot of the forces on the obstacle due to the fluid and to the particles, as a function of the particle eccentricity. This plot shows clearly the importance of the shape of the particles on the result. This figure is for a particle volume fraction of 10^{-4}, which explains why the force due to the fluid is still large compared to the force due to the particles. However, a small increase in particles volume fractions gives a comparable effect for particles and fluid.

If the ratio of densities is smaller, the particles are more completely entrained by the fluid, and follow its trajectory (figure 14).

4.4. Validity of the numerical scheme

Our numerical procedure must be refined where α_l becomes larger, e.g. larger than a few percent. In this case, however, the collisions between particles cannot be neglected, and we must introduce the simulation of these collisions in our code. It is possible to derive a criterion which defines the limit of validity of our procedure. Consider the kinetic energy flux of particles at the boundary of a given cell. Thus,

$$F_p = \alpha_l \rho_l \mathbf{u}_l (\tfrac{1}{2}\mathbf{u}_l^2). \qquad [86]$$

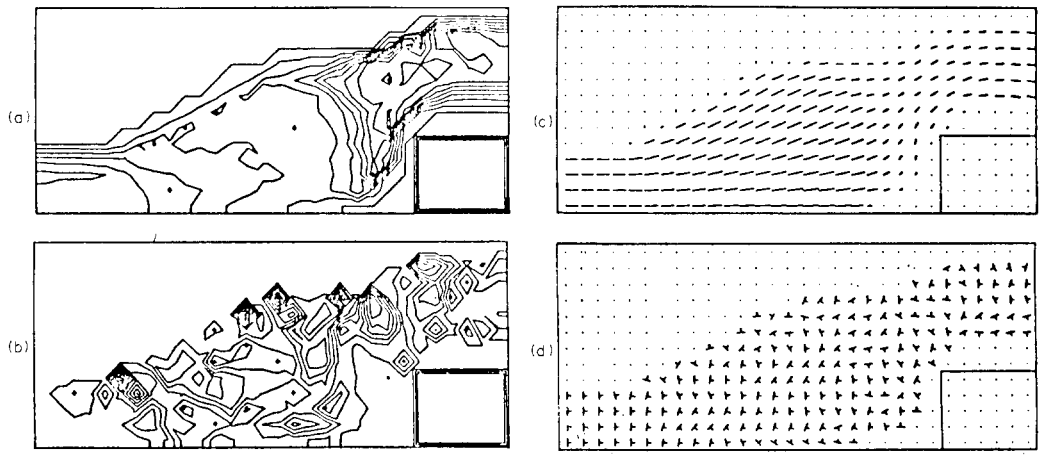

Figure 14. Steady-state patterns: $\rho_1 = 2 \times 10^{-3}$, $\rho_2 = 10^{-3}$, $\alpha_1 = 10^{-3}$, $e = 0.1$, $a = 10^{-3}$. (a) Particles' volume fraction; (b) angular velocity; (c) particles' velocity; (d) particles' orientation.

Similarly, the kinetic energy flux of gas is given by

$$F_g = \alpha_2 \rho_2 \mathbf{u}_2 (\tfrac{1}{2}\mathbf{u}_2^2). \qquad [87]$$

Assume that the particle velocity has already become accommodated to the fluid velocity, $\mathbf{u}_1 = \mathbf{u}_2$. Then the ratio of the two fluxes is $r = \alpha_1 \rho_1 / \alpha_2 \rho_2$. As an example, take $\rho_1 = 1$, $\rho_2 = 10^{-3}$, $\alpha_1 = 10^{-2}$, $\alpha_2 = 0.99$. Here $r = 10$, which shows that even a small particle volume fraction can produce drastic alterations in the flow if the ratio of densities is large enough.

Now consider what happens when the particles enter the shocked region in front of the obstacle. The stopping length for the particles occurs when the particle motion has fluxed out a mass of gas equal to the particle mass. Define l_1 as a characteristic size of the particle and A as its cross-sectional area. The stopping length l_2 is then given by the equation

$$A l_1 \rho_1 = A l_2 \rho_2,$$

where

$$l_2 = l_1 \frac{\rho_1}{\rho_2}. \qquad [88]$$

For example, for spherical particles of radius $a = 10^{-4}$, with the other parameters unchanged $l_2 \simeq 10^3 a$, or $l_2 = 0.1$ cm. In this distance, virtually all the kinetic energy of the particles has been given to the gas, where it resides as heat (which produces a potential energy from which the gas can expand violently). In our example, the gas energy would increase by a factor of 10 when $a = 10^{-6}$, but would only double when $a = 10^{-3}$, the stopping length in this case being made larger than the length of the shocked region. From this analysis, we deduce a criterion for convergence of our numerical procedure. We require that the multiplying factor to gas energy at the front of the obstacle due to the stopping of the particles must be of the order of 1. If D is the shock standoff distance, then the multiplying factor to the gas energy ζ can be expressed as

$$\zeta = \frac{D}{l_2} \frac{\alpha_2 \rho_1}{\alpha_2 \rho_2} \qquad [89]$$

and, since $l_2 = l_1 \rho_1 / \rho_2$, or $l_2 = a \rho_1 / \rho_2$ for spherical particles, we get

$$\zeta \simeq \frac{D}{a} \frac{\alpha_1}{\alpha_2}. \qquad [90]$$

Consider for example the set of parameters: $a = 10^{-4}$, $D = 0.1$, $\alpha_1 = 0.01$, $\alpha_2 = 1$. We obtain $\zeta = 10 \gg 1$, which shows that this criterion is rather restrictive. In such a case, the numerical procedure would have to be changed in the following manner: at the end of an

iteration l, for any variable α_l, we interpolate to obtain the final value of α_l by

$$\alpha_l(\text{final}) = \theta\alpha_l + (1-\theta)\alpha_{l-1}, \qquad [91]$$

θ being a function of ζ such that θ is a decreasing function, and θ tends towards 0 when ζ tends towards infinity.

5. CONCLUSION

The simple model developed in this paper shows the important effects on fluid flow that result from the introduction of nonspherical particles into the flow. These effects differ markedly from those seen when the particles are spherical. For physical cases of interest, such as the rupture of a pipe in a nuclear reactor, or the transport of slurries in a pipeline, the different physical variables are strongly affected and the calculation of exterior wall resistance must take into account the influence of the nonsphericity of the particles. However, we did not account for the deformability of the particles in our model, nor the thermodynamical processes within the particles, which can be predominant in some cases, as shown in our study of relaxation time in section 2. Generalization of our model is very important, and will be presented in a subsequent paper.

NOMENCLATURE

a = Largest half diameter of the spheroids
α_1, α_2 = Volume fractions of particles and fluid
$\mathrm{A}(\beta) = (\cos^2\beta + e^2\sin^2\beta)^{1/2}$
b = Smallest half diameter of the spheroids
β = Angle between the normal to the particle and the relative velocity between the two fields
$\mathrm{B}(\beta) = (\sin^2\beta + e^2\cos^2\beta)^{1/2}$
$C_{\mathrm{L}1}, C_{\mathrm{L}2}$ = Lift force coefficients
γ = Fluid polytropic index
ΔE_{c} = Energy interaction term
ΔE_{p} = Rotational energy interaction term
e = Particles eccentricity
$\mathbf{F}_{\mathrm{D}1}, \mathbf{F}_{\mathrm{D}2}, \mathbf{F}_{\mathrm{D}}$ = Drag force
$\mathbf{F}_{\mathrm{L}1}, \mathbf{F}_{\mathrm{L}2}, \mathbf{F}_{\mathrm{L}}$ = Lift force
F_j = jth component of the force acting on a particle
ΔI_i = Momentum exchange between the two fields
$\mathbb{J}, \mathbb{J}_{ij}$ = Tensor of inertia of a particle
$K_{\mathrm{D}1}, K_{\mathrm{D}2}$ = Drag force coefficients
$K_{\omega 1}, K_{\omega 2}^{\bullet}, K_{\omega 3}, K_{\omega 4}$ = Torque coefficients
m = Mass of a particle
$\mathbf{n}$ = Vector normal to the particle
$N(\mathbf{x}, \mathbf{u}, \mathbf{n}, \boldsymbol{\omega}, t)$ = Particles distribution function
r = Radius of a particle
ρ_1, ρ_2 = Particles and fluid densities
$\rho_1' = \alpha_1\rho_1$
$\rho_2' = \alpha_2\rho_2$
S_{eff} = Cross section of a particle
S_{p} = Particle surface
$\mathbf{T}_1, \mathbf{T}_2, \mathbf{T}_3, \mathbf{T}_4$ = Torque
T_i = Torque ith component
u_{1i}, u_{2i} = ith component of particles and fluid velocities
$\mathbf{U}$ = Relative velocity between the two fields
V_{p} = Particle volume

REFERENCES

BESNARD, D. & HARLOW, F. H. 1985 Turbulence in two-field flows. Los Alamos National Laboratory Report LA-10187-MS.

CHANDRASEKHAR, S. 1943 Stochastic problems in physics and astronomy. *Rev. mod. Phys.* **15,** 1–89.

DALY, B. J. & HARLOW, F. H. 1970 Transport equations in turbulence. *Phys. Fluids* **13,** 2634–2649.

DALY, B. J. & HARLOW, F. H. 1978 Nuclear Regulatory Commission Report No. NUREG/CR-0561; Los Alamos National Laboratory Report No. LA-7610.

GOLDSMITH, H. L. & MASON, S. G. 1962 Flow of suspensions through tubes. I. *J. Colloid Sci.* **17,** 448–476.

JEFFERY, G. B. 1922 Particles immersed in a viscous fluid. *Proc. R. Soc., A* **102,** 161–179.

LAMB, H. 1966 *Hydrodynamics.* Cambridge Univ. Press.

MARGOLIN, L. G. 1977 Ph.D. Thesis; Los Alamos National Laboratory Report LA-7040-T.

NIGMATULIN, R. I. 1979 Spatial averaging in the mechanics of heterogeneous and dispersed systems. *Int. J. Multiphase Flow* **5,** 353–386.

TRAVIS, J. R., HARLOW F. H. & AMSDEN, A. A. 1975 Los Alamos National Laboratory Report LA-5942-MS.